

Prepared for:  
Cape Wind Associates LLC  
75 Arlington Street, Suite 740  
Boston, MA 02116

# Analysis of Effects of Wind Turbine Generator Pile Array for the Alternative Site of the Cape Wind Energy Project

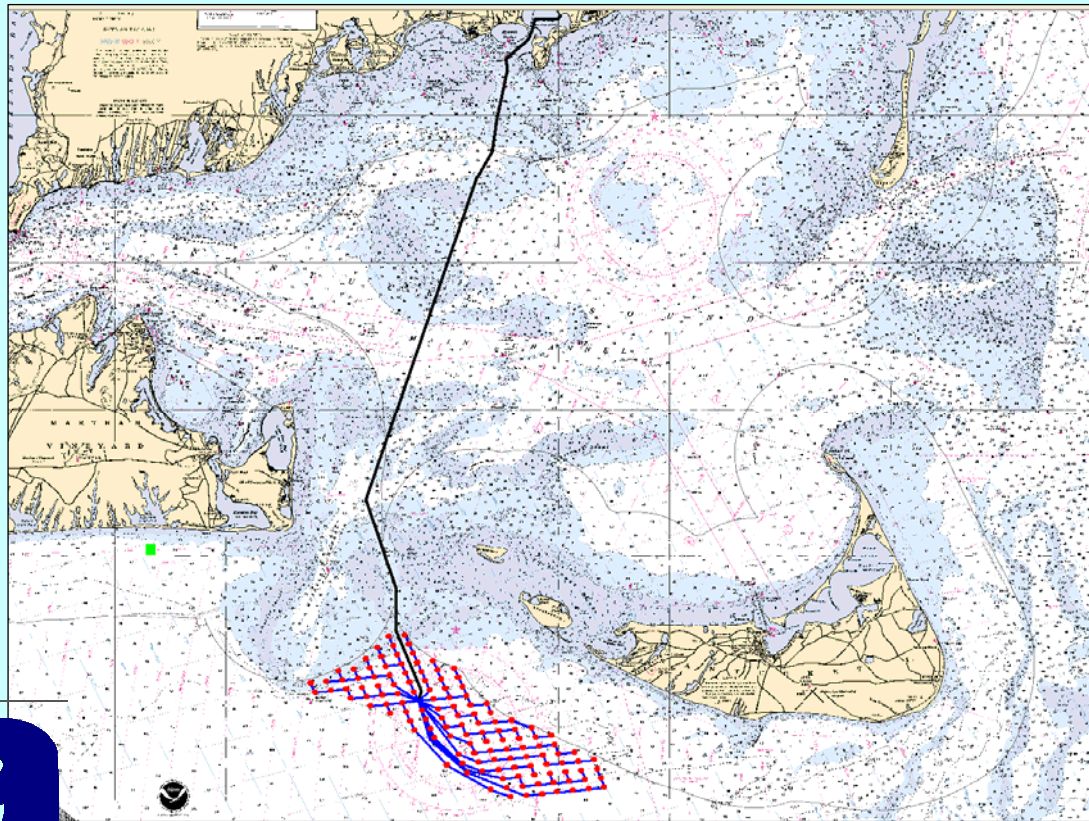
ASA Final Report 05-128

August 2006

Prepared by:  
Craig Swanson  
Sankar Subbayya



Applied Science Associates, Inc.  
70 Dean Knauss Drive  
Narragansett, RI 02882



## Executive Summary

Cape Wind Energy, LLC has proposed to build a wind turbine farm on Horseshoe Shoal in Nantucket Sound. This site has been evaluated in a previous study (Swanson et al., 2005). An alternative site, 9 km (5.6 mi) southwest of Tuckernuck Island, is also being evaluated for comparison purposes. The project will consist of 130 wind turbine generators (WTG), an electric service platform (ESP) and a series of cables connecting the WTGs to the ESP and a pair of cables from the ESP to shore at Yarmouth. Each WTG is either mounted on a monopile or a quad-caisson, consisting of four piles, depending on water depth. Concerns have been raised by regulatory agency review as to the cumulative environmental effects of the WTG pile array on waves and currents and ultimately on sediment transport in Nantucket Sound.

Cape Wind Associates LLC contracted with Applied Science Associates, Inc. to perform an analysis to estimate the expected changes in waves and currents from the placement of the WTG pile array both at the primary site at Horseshoe Shoal and the alternative site southwest of Tuckernuck Island, which is the subject of this report. The study used both a hydrodynamic model, HYDROMAP to calculate currents in the area and wave data collected from the Martha's Vineyard Coastal Observatory (MVCO) to provide input information for the analytic approaches used to estimate the zone of influence of the WTG piles.

The HYDROMAP model was applied to the area offshore Massachusetts and Rhode Island to provide currents in the study area. Details of this application were reported in the analysis of the primary site on Horseshoe Shoal (Swanson et al., 2005).

The monopile analysis approach followed that typically used to evaluate the effects of offshore structures. The key parameters in these analyses are the diffraction parameter, which indicates whether a wave will diffract behind a pile and the Keulegan-Carpenter number, which indicates whether flow around the pile will separate and shed vortices in the downstream direction. Since both parameters require wave length, analysis of one month (December 2003) of wave data (wave height, wave period and water depth) was performed.

Diffraction effects were found to occur for only 4% of the waves from the time series. However the largest diffraction occurred for waves with the smallest period with low induced bottom velocities. These waves cause insignificant sediment transport regardless of whether they diffract or not and so can be ignored.

The calculation of the Keulegan-Carpenter number based on the wave data found no value greater than 3.1, which is only slightly above the threshold (2.8) for flow separation to occur. The mean KC value was approximately 0.96 (with a minimum of 0.19). KC is greater than 2.8 only 0.6 % of the month. The data primarily falls within the zone of insignificant separation effects (low KC) and insignificant diffraction (low D/L).

A potential flow analysis appropriate for this condition shows that the flow around the pile returns to within 89% of its undisturbed value within 1 pile diameter from the pile and to within 99% of its undisturbed value within 4 pile diameters. Using the same approach for the periodic tidal wave, a very long period shallow water wave, gave a large KC value of 3800, indicating that vortex shedding would occur. The velocity defect created by this vortex street dissipates rapidly, however, scaling at  $x^{-2/3}$ , where x is the distance downstream.

Comparison to laboratory studies of multiple piles indicates that there is no anticipated wake interaction among the piles since interaction ceases when the piles are spaced greater than five

pile diameters from each other and the spacing for this project ranges from 120 to 190 pile diameters. Using a single pile zone of influence of 5 pile diameters long (if not significantly shorter) and 2 diameters wide or less than 280 m<sup>2</sup> (3014 ft<sup>2</sup>), the total area for all 130 piles is less than 0.0364 km<sup>2</sup> (9 ac). This area can be compared to the total area of the WTG pile array on Horseshoe Shoal of 71 km<sup>2</sup> (17,500 ac) showing that only 0.051% of the area is potentially affected. In reality, only a very small portion of this area is actually affected since all these impacts decrease quickly away from the pile.

An analysis of scour around quad caisson configuration followed two approaches. The first looked at the literature for pile groups and found that the pile spacing to pile diameter (G/D) ratio was the critical parameter besides the KC number. The proposed quad caisson design ranged from 1.7 to 2.9 depending on the angle of the waves and currents impinging on the structure. Laboratory experiments showed that G/D ratios greater than 1 to 2, depending on pile group configurations, showed no interference effects among the piles. Thus for the most sensitive orientation of waves and currents oriented toward a corner of the quad caisson there may be an increased scour effect of approximately 20% over single pile results.

The second approach assumed that an equivalent monopile pile diameter can be calculated from a pile group based on the angle of attack of the flow, the individual pile diameter and the pile spacing. For the quad caisson geometry, the projected equivalent pile diameter is 11.3 m (37 ft). This results in an equivalent pile diameter 2.1 times the diameter of the average monopile used in shallower water. This approach resulted in a maximum possible pile effects area less than 1280 m<sup>2</sup> (13,800 ft<sup>2</sup>). If one conservatively assumes that all 130 piles use the quad-caisson configuration for this site, less than 0.166 km<sup>2</sup> (41 ac) can be compared to the total area of the wind farm of 71 km<sup>2</sup> (17,500 ac) showing that only 0.23 % of the area of the wind farm is potentially affected. Even though larger than the monopile results, the equivalent pile diameter approach still results in only a very small portion of the wind farm area is actually affected.

# Table of Contents

Executive Summary ..... i

Table of Contents.....iii

List of Figures..... iv

1 Introduction ..... 1

2 Description of the Study Area and Project ..... 2

3 HYDROMAP Hydrodynamic Model..... 4

    3.1 HYDROMAP Application ..... 4

    3.2 HYDROMAP Model Results ..... 5

4 Analysis of WTG Piles on Waves and Currents..... 7

    4.1 Analytical Approach..... 7

    4.2 Application to Wind Farm Site ..... 9

    4.3 Analysis Results ..... 13

        4.3.1 Monopile Design ..... 13

        4.3.2 Quad-Caisson Design ..... 18

5 Conclusions..... 20

6 References..... 22

## List of Figures

Figure 2.1 Location of alternate wind farm site southwest of Tuckernuck Island showing WTGs as red circles, WTG connecting cables as thin blue lines and main power cable to shore as thick black line. Horseshoe Shoal, the primary wind farm location, is also shown. ....	3
Figure 3.1 Hydrodynamic model grid cells for entire HYDROMAP domain.....	4
Figure 3.2 Hydrodynamic model grid depths for entire HYDROMAP domain.....	5
Figure 3.3 M2 flood vectors at alternative wind farm site. Scale of vectors shown in upper left corner as 1 kt (0.5 m/s).....	6
Figure 3.4 M2 ebb vectors at alternative wind farm site. Scale of vectors shown in upper left corner as 1 kt (0.5 m/s). ....	6
Figure 4.1 Schematic to show what wave force regimes one is located in for a given selection of KC (shown as K in the figure), D/L and H/L. Graphic from Isaacson (1979) as shown in Sarpkaya and Isaacson (1981). ....	8
Figure 4.2 December 2003 time series of surface elevation from MVCO site.....	10
Figure 4.3 December 2003 time series of wave heights from MVCO site.....	11
Figure 4.4 December 2003 time series of wave periods from MVCO site.....	11
Figure 4.5 Time series of calculated wave lengths based on observations from the MVCO site. ....	12
Figure 4.6 Time series of wave height to length ratios based on observations from the MVCO site. ....	12
Figure 4.7 December 2003 time series of diameter to wavelength, D/L.....	14
Figure 4.8 Wave height as a function of wave period from MVCO observations. ....	14
Figure 4.9 Wave period as a function of diffraction parameter, D/L. ....	15
Figure 4.10 December 2003 time series of Keulegan-Carpenter number.....	15
Figure 4.11 Relationship of KC and D/L for December 2003 observations from MVCO site. ....	16
Figure 4.12 Velocity variation based on potential flow in downstream and cross stream directions. ....	17

# 1 Introduction

Cape Wind Energy, LLC has proposed to build a wind turbine farm on Horseshoe Shoal in Nantucket Sound. This site has been evaluated in a previous study (Swanson et al., 2005). An alternative site, 9 km (5.6 mi) southwest of Tuckernuck Island, is also being evaluated for comparison purposes. The project will consist of 130 wind turbine generators (WTG), an electric service platform (ESP) and a series of cables connecting the WTGs to the ESP and a pair of cables from the ESP to shore at Yarmouth. Each WTG is either mounted on a monopile or a quad-caisson, consisting of four piles, depending on water depth. Concerns have been raised by regulatory agency review as to the cumulative environmental effects of the WTG pile array on waves and currents and ultimately on sediment transport in Nantucket Sound.

Cape Wind Associates LLC contracted with Applied Science Associates, Inc. to perform an analysis to estimate the expected changes in waves and currents from the placement of the WTG pile array both at the primary site at Horseshoe Shoal and the alternative site southwest of Tuckernuck Island, which is the subject of this report. The study used both a hydrodynamic model, HYDROMAP to calculate currents in the area and wave data collected from the Martha's Vineyard Coastal Observatory (MVCO) to provide input information for the analytic approaches used to estimate the zone of influence of the WTG piles.

ASA's HYDROMAP model was applied to the area offshore Massachusetts and Rhode Island to predict the currents necessary as input to the pile effects analysis. The model uses a variable grid size capability to provide model predictions of currents for sufficient resolution. HYDROMAP was driven by tides at its open boundaries and predicted tidal elevations and currents in the area. More details are found in Swanson et al. (2005). A series of analyses were then conducted to assess the zone of influence of the WTG pile array based on its effects on waves and currents.

This report documents the model application and analyses of the extent of the WTG pile array in waves and currents at the alternate wind farm site southwest of Tuckernuck Island. Section 1 presents the introduction to the study. Section 2 describes the study area and project. Section 3 presents the HYDROMAP model used to simulate currents and its application and results. Section 4 presents the pile effects analysis on waves and currents. Section 5 provides conclusions from the study and Section 6 lists references.

## 2 Description of the Study Area and Project

The proposed primary wind energy project site is to be located on Horseshoe Shoal in Nantucket Sound (Figure 2.1). Details of the analysis of that site are presented in Swanson et al. (2005). The alternative site, the subject of the analysis in this report, is located 9 km (5.6 mi) southwest of Tuckernuck Island, which is located just west of Nantucket Island (Figure 2.1). The site lies just outside of Nantucket Sound to the south in the Atlantic Ocean. The depths relative to Mean Lower Low Water (MLLW) range from 3.6 m (12 ft) to 27 m (90 ft) at the site based on NOAA Chart 13237.

The Wind Park at the alternative location south of Tuckernuck Island will consist of 130 wind turbine generators (WTG), an electric service platform (ESP) and a series of cables connecting the WTGs to the ESP and two cable circuits from the ESP to a landfall in Yarmouth on Cape Cod (Figure 2.1). The turbines will be located in an array designed to maximize energy production. Each WTG is mounted on a monopile or a quad-caisson, consisting of four piles, driven into the seabed. The monopile is between 5.1 and 5.5 m (16.75 and 18 ft) in diameter at the MLLW water line. The smaller diameter will be used in water depths from 3.6 to 12 m (12 to 39 ft) MLLW while the larger diameter will be used between depths of 12.2 to 15.2 m (40 to 50 ft). The quad-caisson consists of four piles 7.5 m (24.6 ft) in diameter tied together with cross members and connected to the tower supporting the WTG. The quad-caisson piles are located on the corners of a square 29 m (95 ft) on a side measured from the centerline of each pile. The quad-caisson design will be used in water depths from 15.2 to 27 m (50 to 90 ft). The spacing between the WTGs is approximately 0.63 km (0.34 nm) in the generally north / south direction and 1 km (0.54 nm) in the generally east / west direction.

The ESP is located near the center of the WTG array and is the termination point of all the 33kV cables from the WTGs and the two 115kV cables from shore. It is a fixed platform on six 107 cm (42 in) diameter piles driven into the seabed. Water depth at the site is 28 m (78 ft) MLLW. The cables connecting the WTGs to the ESP vary in diameter from 132 mm (5.2 in) to 164 mm (6.5 in) depending on the number of WTGs to which they are connected (up to 10) and are rated at 33kV.

The cables are to be buried to a minimum depth of 1.8 m (6 ft) below present bottom using a jetting technique whereby pressurized seawater is jetted into the seabed to fluidize the sediments along the cable route. The cable then sinks of its own weight through the fluidized sediments and is buried as the sediment returns to its pre-jetted condition. It is estimated that the fluidized trench created by the jetting process is approximately 1.8 m (6 ft) wide at the seabed, 2.4 m (8 ft) deep and 0.6 m (2 ft) wide at the bottom. The jetting equipment moves at approximately 91 m/hr (300 ft/hr).

Data for this analysis was obtained from the Martha's Vineyard Coastal Observatory (MVCO) which is located in Edgartown, Massachusetts. The project was initiated by the Woods Hole Oceanographic Institution to study coastal atmospheric and oceanic processes. The MVCO includes an underwater node located at the 12-m (39-ft) isobath shown in Figure 2.1. The node instrumentation is connected directly to a shore lab via a buried electro-optic power cable. The oceanographic sensors measure current profiles, waves, temperature and salinity. The website address from which the data was downloaded is <http://www.whoi.edu/mvco/data/oceandata.html>.

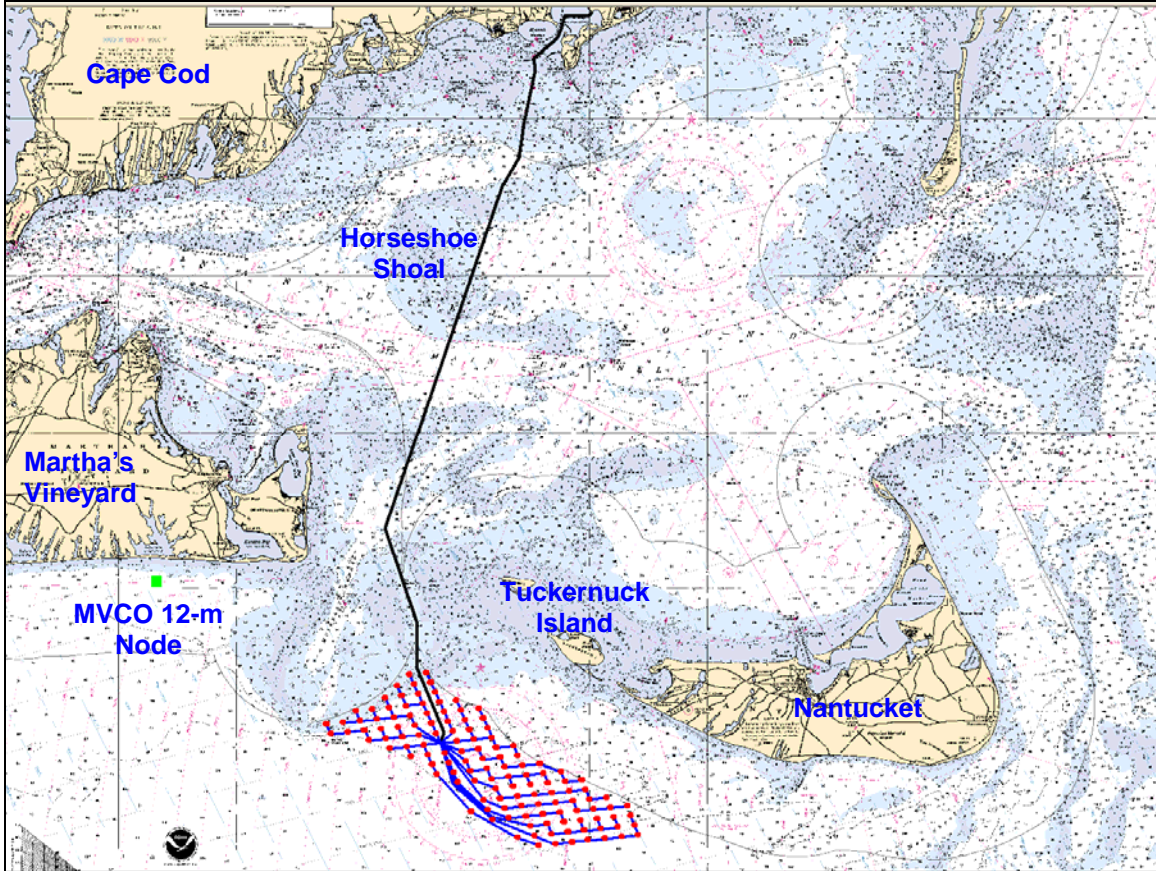


Figure 2.1 Location of alternate wind farm site southwest of Tuckernuck Island showing WTGs as red circles, WTG connecting cables as thin blue lines and main power cable to shore as thick black line. Horseshoe Shoal, the primary wind farm location, is also shown.



### 3 HYDROMAP Hydrodynamic Model

HYDROMAP is a globally re-locatable hydrodynamic model (Isaji, et al., 2001) capable of simulating complex circulation patterns due to tidal forcing, wind stress and fresh water flows quickly and efficiently anywhere on the globe. Description of the model and details of its application to the southern New England coastal waters, as part of the analysis of the primary location, Horseshoe Shoal within Nantucket Sound, is found in Swanson et al. (2005).

#### 3.1 HYDROMAP Application

The southern New England coastal area is a complex topographic and bathymetric area which results in a complex current velocity structure. In order to account for this complexity the hydrodynamic model domain extended to deep waters (~200 m [660 ft]) in the south and east directions, to Block Island in the west direction and to the north end of Massachusetts Bay in the north direction. Figure 3.1 shows the computational model grid cells for the entire domain. At the open boundary and in the outer regions, a maximum cell size of ~2.5km (~1.6 mi) was assigned. Cell resolution was gradually increased toward Nantucket Sound, based on the primary site on Horseshoe Shoal, where a uniform cell size of 315 m (~1,030 ft) was employed. The alternative site south of Tuckernuck Island has a slightly larger cell size of 630 m (2060 ft), but adequate to represent the currents in that area.

The bathymetry data used in the model grid was assembled from various sources: survey data (supplied by Cape Wind Associates), the hydrographic survey data CD-ROM Set (NGDC 1998), and ETOPO2 (NGDC 2001). Figure 3.2 shows the bathymetry used in the model.

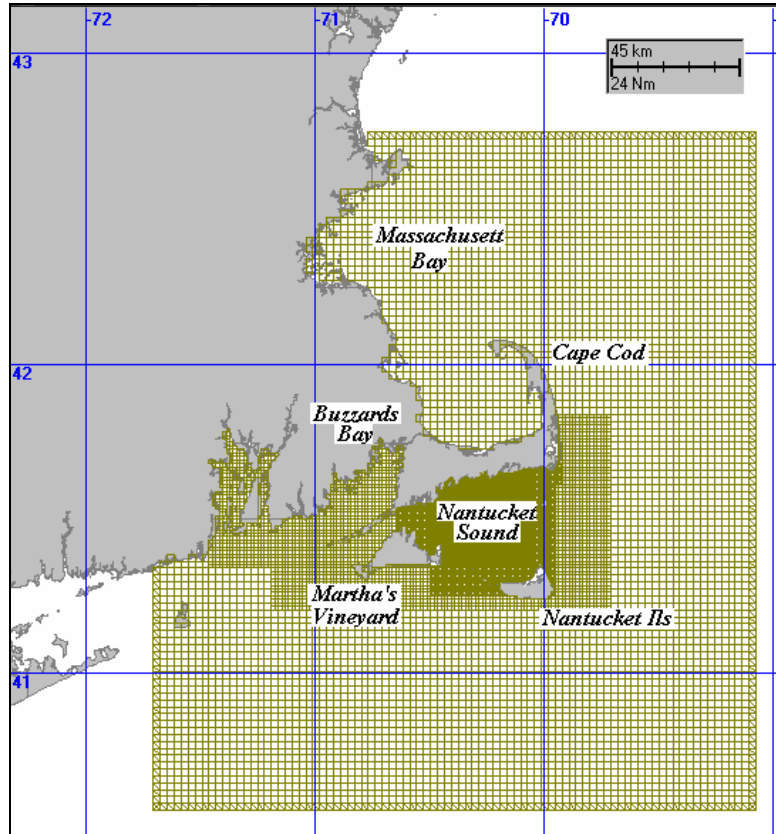


Figure 3.1 Hydrodynamic model grid cells for entire HYDROMAP domain.

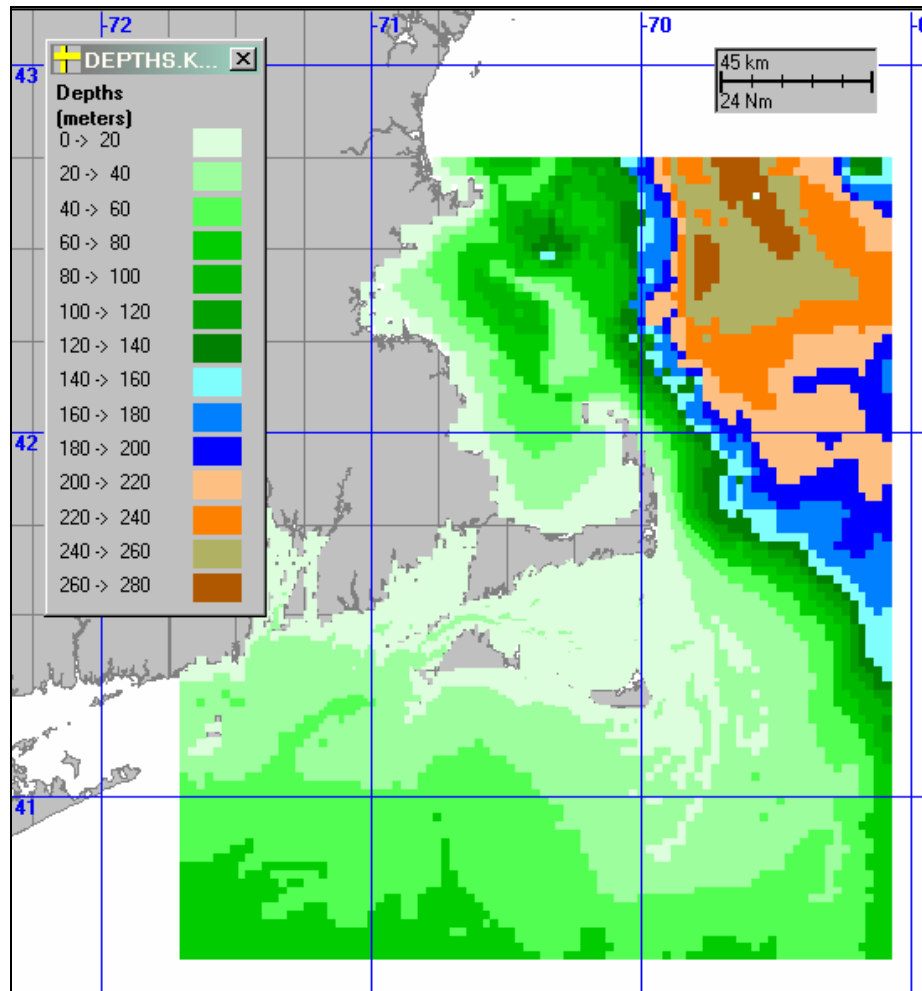


Figure 3.2 Hydrodynamic model grid depths for entire HYDROMAP domain.

### 3.2 HYDROMAP Model Results

The HYDROMAP model was successfully calibrated based on a comparison of multiple tidal constituents at various locations around Nantucket Sound. Details of the calibration process are found in Swanson et al. (2005).

Figures 3.3 and 3.4 show the predicted M2 tidal flood and ebb currents in the alternative site area, respectively. Currents flow primarily northward on flood and southward on ebb on the shallow areas just north of the site. Highest speeds, ( $\sim 0.5$  m/s [ $\sim 1$  kt]) occur at the northwestern portion of the wind farm site. Currents at the wind farm site, located in deeper water, flow generally to the northeast or east at  $\sim 0.25$  m/s ( $\sim 0.5$  kt) on flood and south or southwest at  $\sim 0.20$  m/s ( $\sim 0.4$  kt) on ebb. The large variation in depths below the wind farm site is clearly seen in these figures.

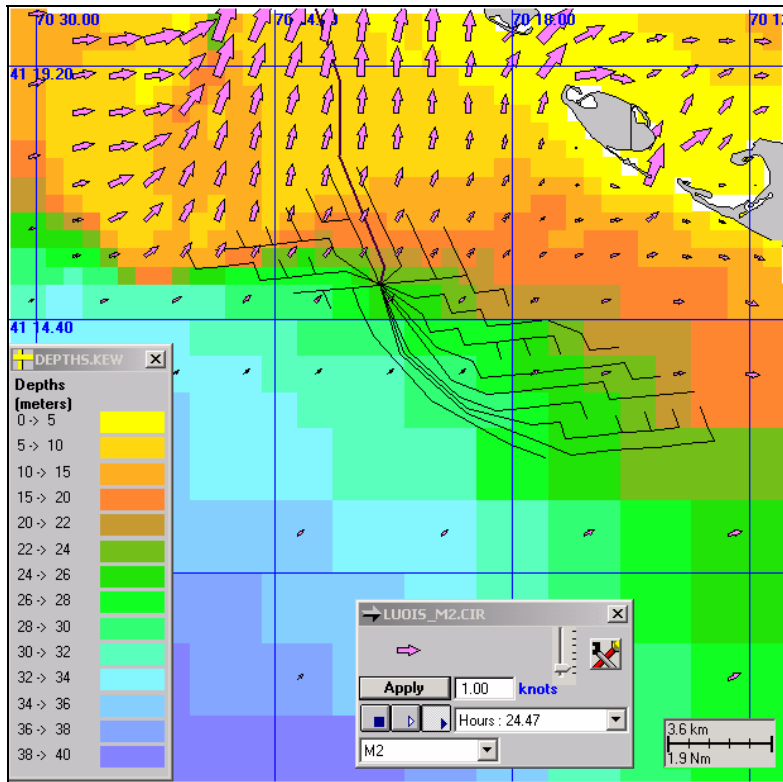


Figure 3.3 M2 flood vectors at alternative wind farm site. Scale of vectors shown in upper left corner as 1 kt (0.5 m/s).

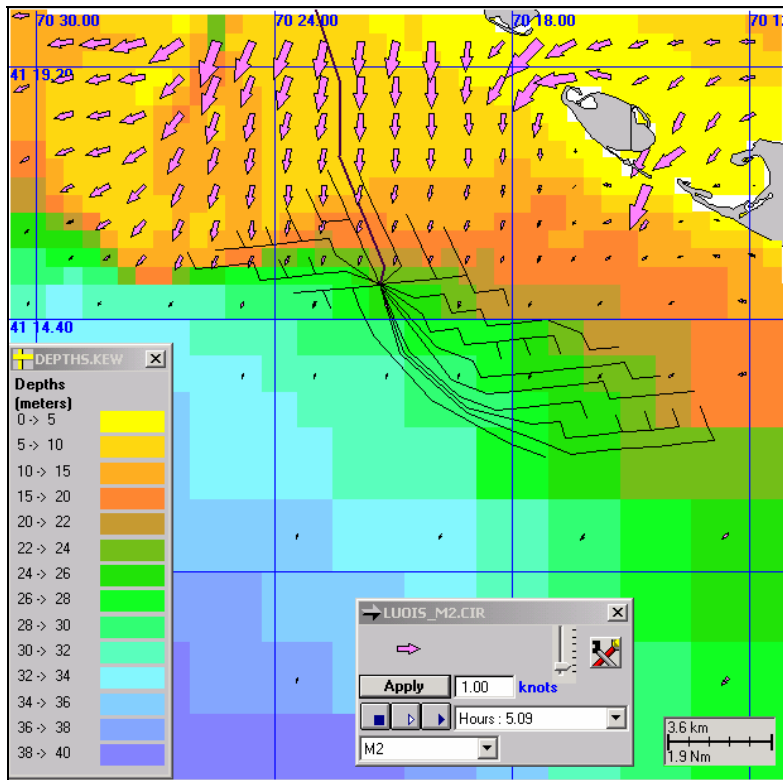


Figure 3.4 M2 ebb vectors at alternative wind farm site. Scale of vectors shown in upper left corner as 1 kt (0.5 m/s).

## 4 Analysis of WTG Piles on Waves and Currents

### 4.1 Analytical Approach

Concern has been raised about the potential effects of the array of WTG monopiles on currents and waves and ultimately on sediment transport at the alternative wind farm site southwest of Tuckernuck Island. This area experiences active sediment transport based on the presence of coarse grain sediments found. The approach presented is to assess the zone of influence of a single pile and then evaluate the potential interaction of multiple piles to determine the cumulative zone of influence. This analytical approach is the same as that used for the primary wind farm site on Horseshoe Shoal in Nantucket Sound (Swanson et al., 2005).

To determine if a larger cumulative area would be affected, the work of Sarpkaya and Isaacson (1981) which examines the effects of waves and currents on offshore structures was followed. There are four parameters that define flow and wave regimes around piles. The first is the water depth to wavelength ratio,  $h/L$ . This parameter is used to determine whether a wave can be considered a deep, transitional, or shallow water wave. The second is the wave height to wavelength ratio,  $H/L$ , which describes wave steepness. If wave steepness is small ( $H/L < 1/10$ ), as will be shown below, the linear wave approximation can be applied, simplifying the analysis with no loss of accuracy. The third parameter is the pile diameter to wavelength ratio,  $D/L$ , also known as the diffraction parameter. Diffraction is the process where the wave front bends around an object thus propagating wave energy behind the pile. The fourth is the Reynolds number, which is defined as the ratio of viscous effects to inertia effects on the pile, and is expressed as

$$Re = UD/\nu$$

where  $U$  is a characteristic velocity and  $\nu$  is the kinematic viscosity of water.

There are two flow regimes around a pile depending on pile size (Sumer and Fredsoe, 2002) or diffraction parameter,  $D/L$ . The first is known as the slender pile regime where the pile diameter is so small or the wavelength is so large that the flow separates from the pile and forms a zone of attached or shedding vortices behind the pile. The characteristics of this zone are governed by the Reynolds number. For  $Re < \sim 7$ , the flow does not separate and potential flow theory applies. Flow separation behind a cylinder with re-circulating eddies occurs at about  $Re = 7$  and continues up to about  $Re = 60$  when the eddies begin to alternately separate and form a von Karman vortex street (White, 1991). For the problems of interest here, the  $Re$  is large ( $Re \sim 100$ ) and the flow will separate and result in a turbulent wake downstream of the pile.

When the diffraction parameter is relatively small, however, the Keulegan-Carpenter number has more physical significance. It is simply an extension of the flow separation problem to unsteady (oscillatory) flows and is defined as the ratio of the characteristic wave dimension divided by diameter or

$$KC = U_m T_w / D$$

where  $U_m$  is the maximum orbital wave velocity and  $T_w$  is the wave period. Assuming sinusoidal waves,  $KC$  can also be expressed as

$$KC = 2\pi a / D$$

where  $a$  is the amplitude of the orbital motion (or where  $2a$  is the stroke). Large values of  $KC$  mean that the orbital motion is large relative to pile diameter.

Figure 4.1 is a schematic to show which wave force regime applies for a given  $KC$ ,  $D/L$ , and  $H/L$ . This figure indicates the conditions when flow separation is important (for increasing  $KC$ ), when diffraction is important (for  $D/L > 0.2$  [Isaacson, 1979]) and when nonlinear effects become important.

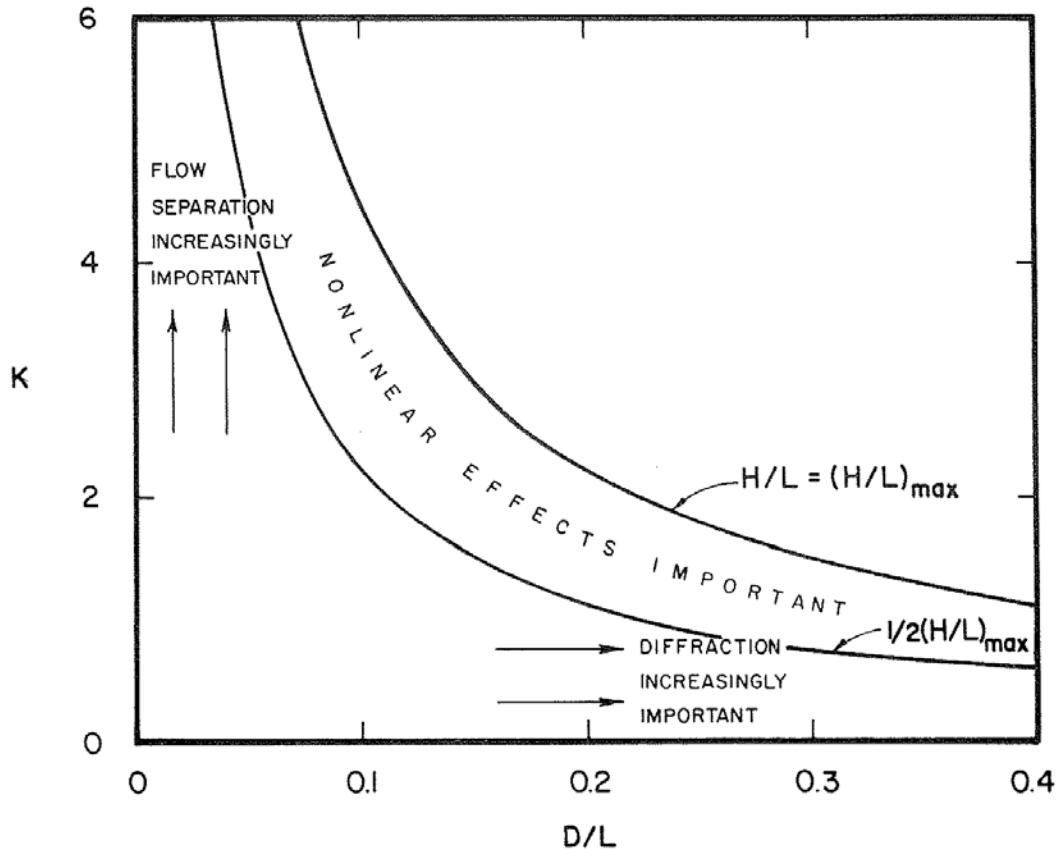


Figure 4.1 Schematic to show what wave force regimes one is located in for a given selection of  $KC$  (shown as  $K$  in the figure),  $D/L$  and  $H/L$ . Graphic from Isaacson (1979) as shown in Sarpkaya and Isaacson (1981).

The amplitude of the wave velocity at the surface based on linear theory is

$$a = \frac{H/2}{\tanh(2\pi h/L)}$$

where  $H$  is the wave height and  $h$  the water depth. The Keulegan-Carpenter number can thus be written as

$$KC = \frac{\pi(H/L)}{(D/L) \tanh(2\pi h/L)}$$

The Keulegan-Carpenter number controls the generation of wake vortices. Sumer et al. (1997) presents the following regimes:

- $KC < 2.8$ . No flow separation occurs behind the cylinder. The flow around the pile is governed by potential flow theory.

- $2.8 < KC < 4$ . Flow separation occurs behind the cylinder with re-circulating vortices. They move around the cylinder as the wave velocity reverses.
- $4 < KC < 6$ . The vortices become asymmetric but do not shed.
- $KC > 6$ . The vortices shed resulting in a lee wake behind the pile.

The second regime is known as the large pile regime where the pile diameter is so large or the wavelength is so small that there is no separation zone but waves are diffracted behind the pile. From Figure 4.1, diffraction is only important for very short period waves whose wavelengths are comparable to the pile diameter (for  $D/L > 0.2$ ).

## 4.2 Application to Wind Farm Site

The application of the approach presented in the previous section requires data on the wave and current environment at the WTG array. Predicted currents from the HYDROMAP application described in Section 3 were used as were wave measurements from the MVCO 12-m node site. The MVCO data includes 20-min time series of wave height and period as well as surface elevation. The determination of wave length based on these parameters must be made before the analysis outlined above can be performed.

The wavelength,  $L$ , for a given water depth,  $h$ , and wave period,  $T$ , can be obtained by solving the transcendental equation describing linearized water waves that are periodic in space and time propagating over a flat bottom,

$$\sigma^2 = gk \tanh(kh)$$

where  $\sigma = 2\pi/T$ ,  $g$  is the acceleration due to gravity, and  $k = 2\pi/L$ . Hunt (1979) presented an approximate solution for this equation in terms of  $kh$  which is accurate to 0.1% as,

$$(kh)^2 = y^2 + \frac{y}{1 + \sum_{n=1}^6 d_n y^n}$$

where  $y = h\sigma^2/g$  and the constants are:  $d_1 = 0.6666666666$ ;  $d_2 = 0.3555555555$ ;  $d_3 = 0.1608465608$ ;  $d_4 = 0.0632098765$ ;  $d_5 = 0.0217540484$ ; and  $d_6 = 0.0065407983$ .

A representative month-long data set for December 2003 was used in the calculation of the wavelength,  $L$ . This time period is the same as that used for the original analysis for the primary Horseshoe Shoal site. Figures 4.2 through 4.4 show the time series of surface elevation, wave height and wave period, respectively, for the month from the MVCO 12-m node site. Some data gaps are evident in the record as shown but this missing data, 131 points out of a total of 2220, are not significant in the analysis presented here. A 1-hr filter was applied to the data. The predominant M2 tidal variation is clearly seen in Figure 4.2 with periodic offsets due to setup and setdown from the wind. Mean tide range is  $\sim 1$  m ( $\sim 3.3$  ft).

Water depth at the MVCO site is 12 m (39 ft) and was assumed to be representative of the range of site depths (3.6 to 27 m [12 to 90 ft]).

Figure 4.3 shows the variation of wave height to be related to events of one to three days duration. Wave heights ranged from 0.3 to 3.5 m (1 to 11.5 ft) with an average of 1.42 m (4.66 ft).

Figure 4.4 presents wave period, which generally shows a positive correlation with wave height. Periods range from 3.5 to 9.5 sec during the month. The average period for the month was 6.0 sec.

Figure 4.5 shows the calculated wave length which is directly correlated with the wave period. The wavelengths range from 19 to 94 m (62 to 308 ft) with an average of 50 m (164 ft).

Figure 4.6 shows the wave height to length ratio for the month. The linear wave assumption is shown to be valid since all H/L values are less than 0.1.

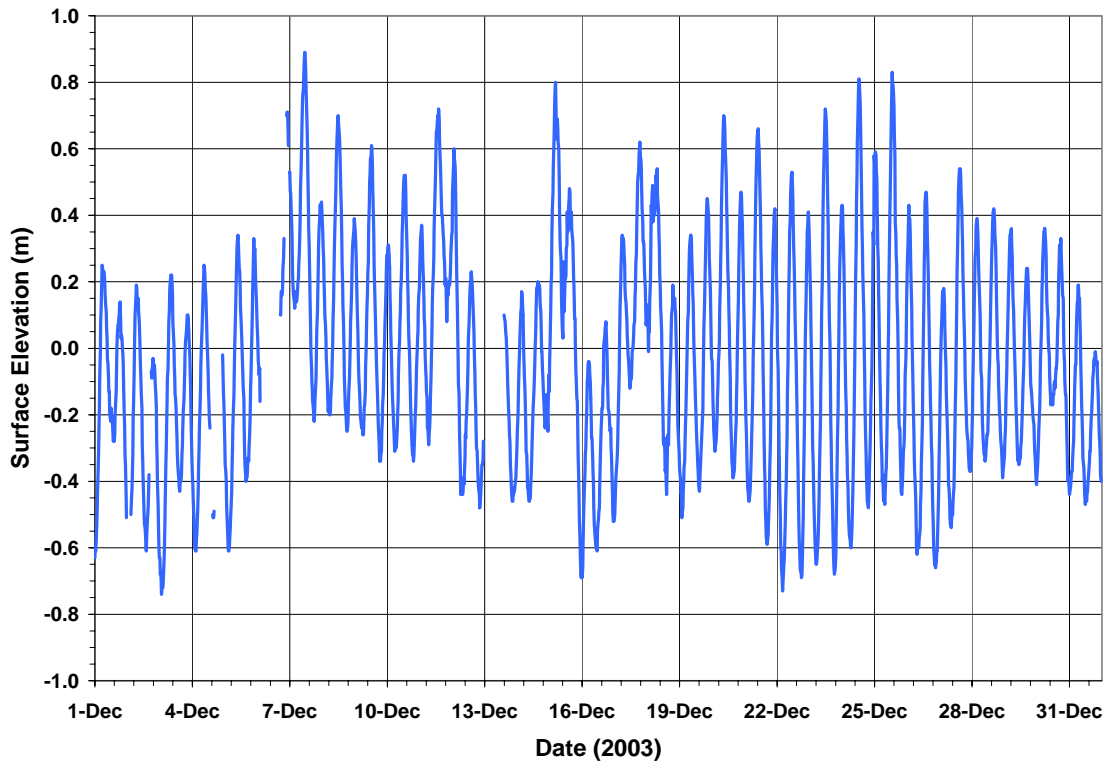


Figure 4.2 December 2003 time series of surface elevation from MVCO site.

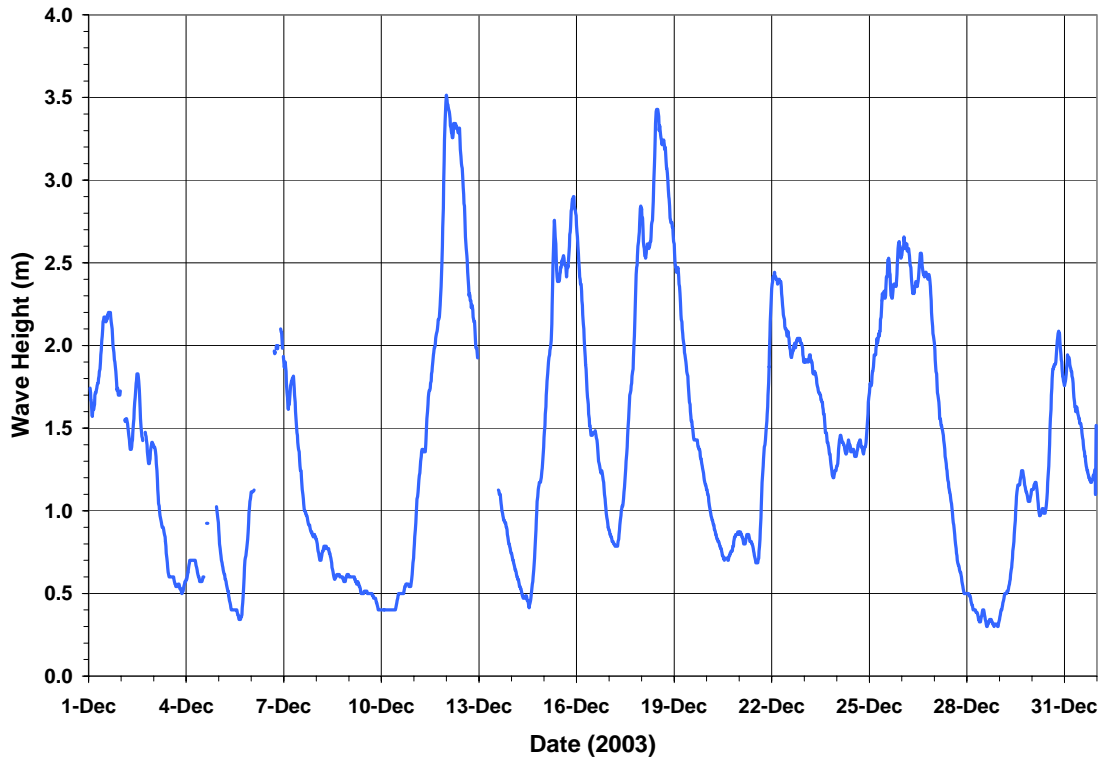


Figure 4.3 December 2003 time series of wave heights from MVCO site.

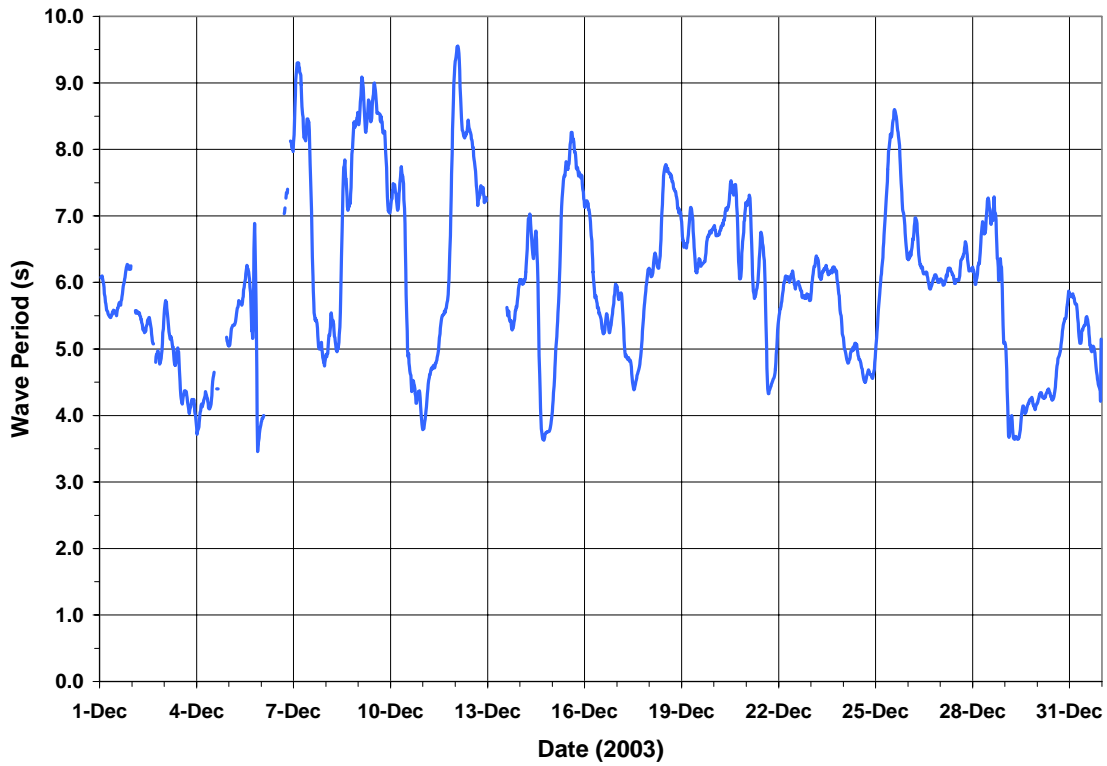


Figure 4.4 December 2003 time series of wave periods from MVCO site.



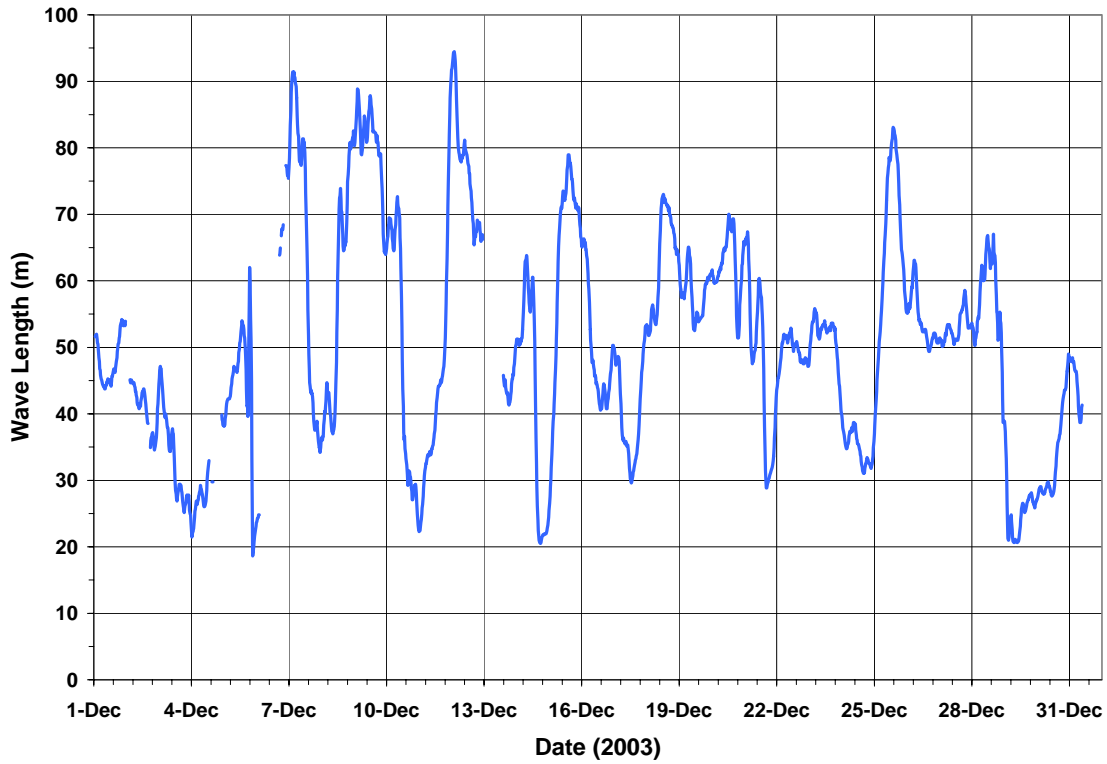


Figure 4.5 Time series of calculated wave lengths based on observations from the MVCO site.

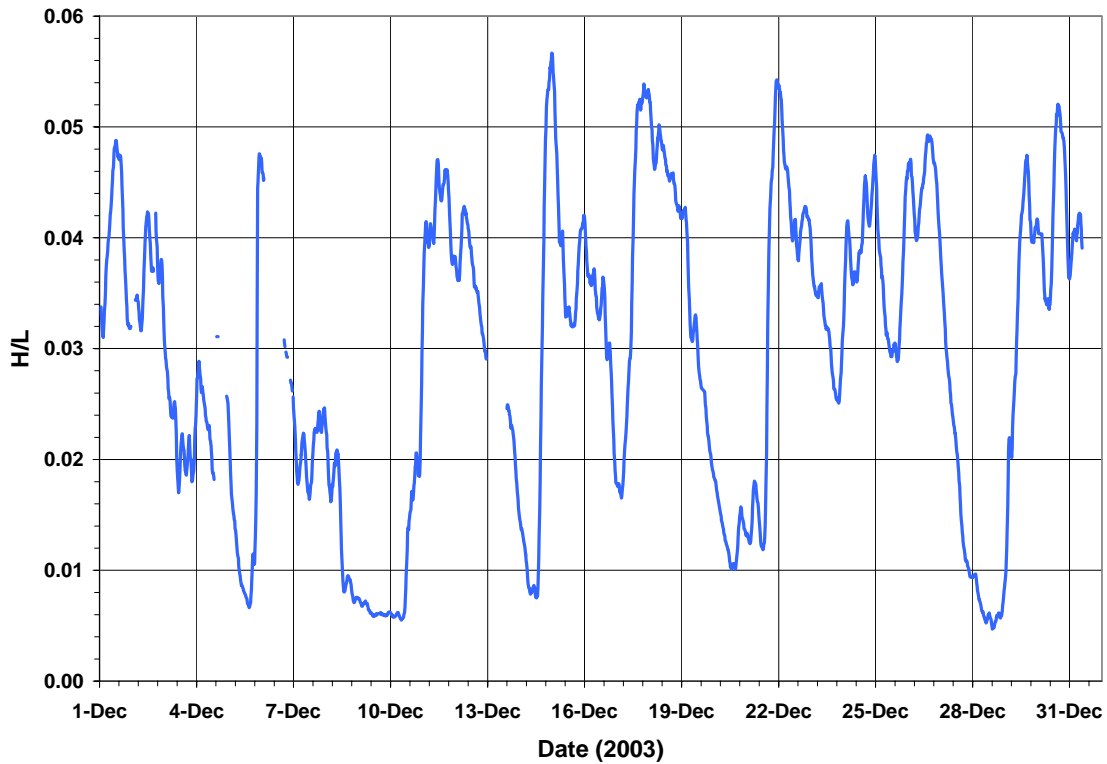


Figure 4.6 Time series of wave height to length ratios based on observations from the MVCO site.

## 4.3 Analysis Results

Using the wave observations from the MVCO and the calculated wavelength, time series of the diffraction parameter and Keulegan-Carpenter number were calculated to determine whether separation or diffraction effects are important (Figure 4.1) and estimates of changes in currents and velocity made. The results for the monopile design are presented in Section 4.3.1. Extension of the analysis for the quad-caisson design is presented in Section 4.3.2

### 4.3.1 Monopile Design

An average monopile diameter of 5.3 m (17.4 ft) was used in these calculations since the range of diameters is only 5.1 to 5.5 m (16.75 to 18 ft). Figure 4.7 shows the resulting time series of the D/L ratio based on the December 2003 wave data. From the previous section, a D/L ratio less than 0.2 indicates diffraction effects are insignificant and the piles are essentially invisible to the waves. For the time series presented here a D/L ratio  $< 0.2$  occurs 94% of the time. The maximum D/L ratio of 0.28 is due to the minimum measured period of 3.5 sec with a wave height of 0.3 m (1 ft). These short-period waves have very low induced bottom velocities so their effect on sediment transport is insignificant.

Figure 4.8 shows the relationship between wave height and wave period. The range of wave height increases with wave period, i.e., from a range of 0.5 to 1 m (1.6 to 3.3 ft) at 3.5 sec to a range of 0.5 to 3.5 m (1.6 to 11.5 ft) at 9 sec.

Figure 4.9 shows the relationship between wave period and diffraction parameter. Waves for which diffraction is important ( $D/L > 0.2$ ) are short period waves ( $< 4$  sec). Only four percent of the waves are in this category.

A time series of the Keulegan-Carpenter number was then calculated to determine if separation effects due to waves are important (Figure 4.10). The KC value ranges from 0.19 to 3.1 with a mean value of approximately 0.96, typically much less than the KC minimum where separation occurs ( $KC > 2.8$ ). KC is greater than 2.8 only 0.6 % of the month. Figure 4.11 shows the actual relationship of KC to D/L (shown conceptually in Figure 4.1) for the observations and calculated wavelength. The data primarily falls within the zone of insignificant separation effects (low KC) and insignificant diffraction (low D/L) as discussed above.

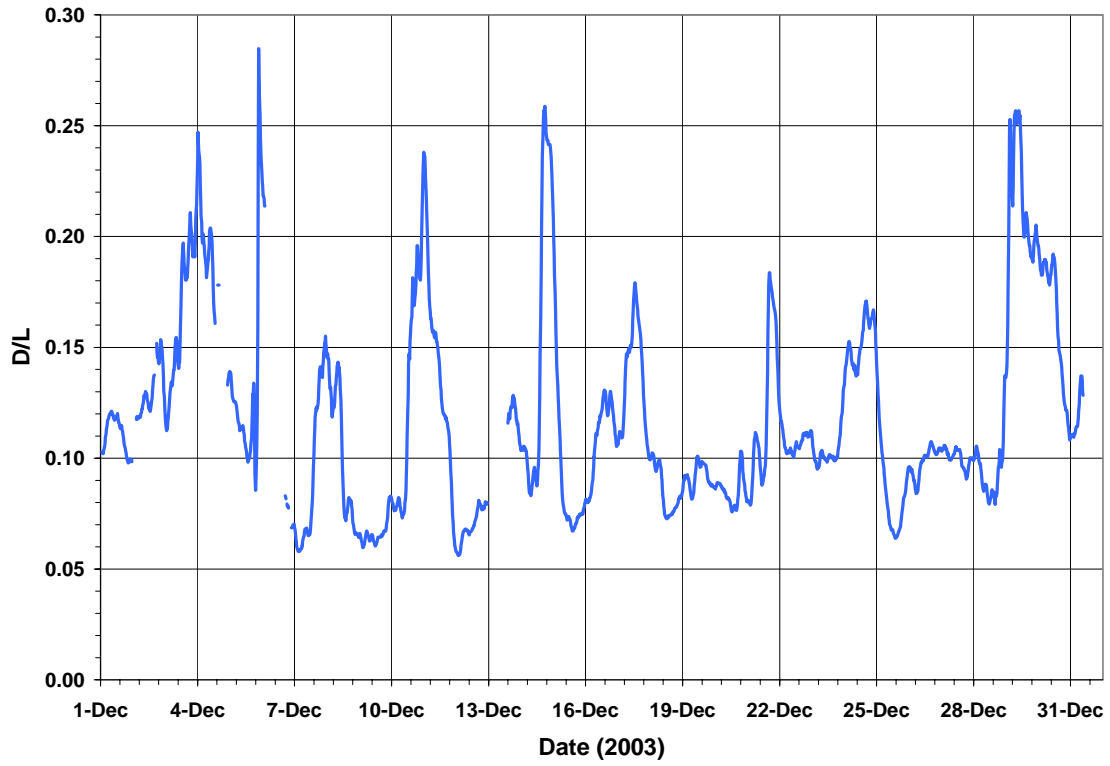


Figure 4.7 December 2003 time series of diameter to wavelength, D/L.

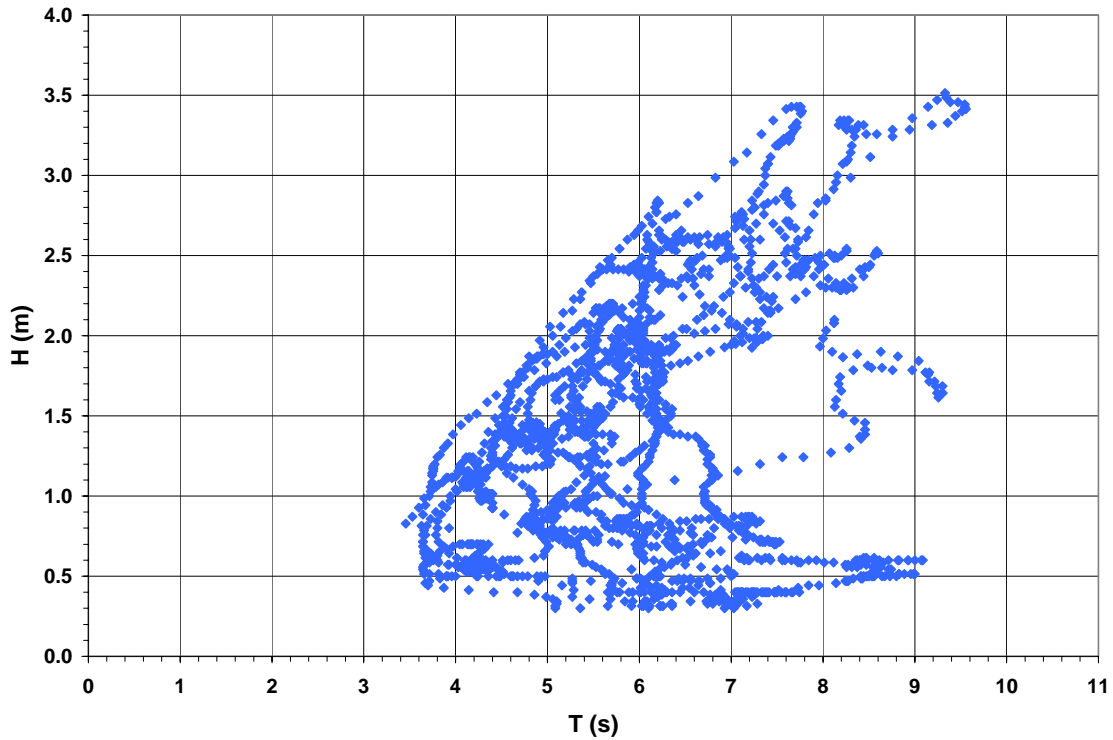


Figure 4.8 Wave height as a function of wave period from MVCO observations.

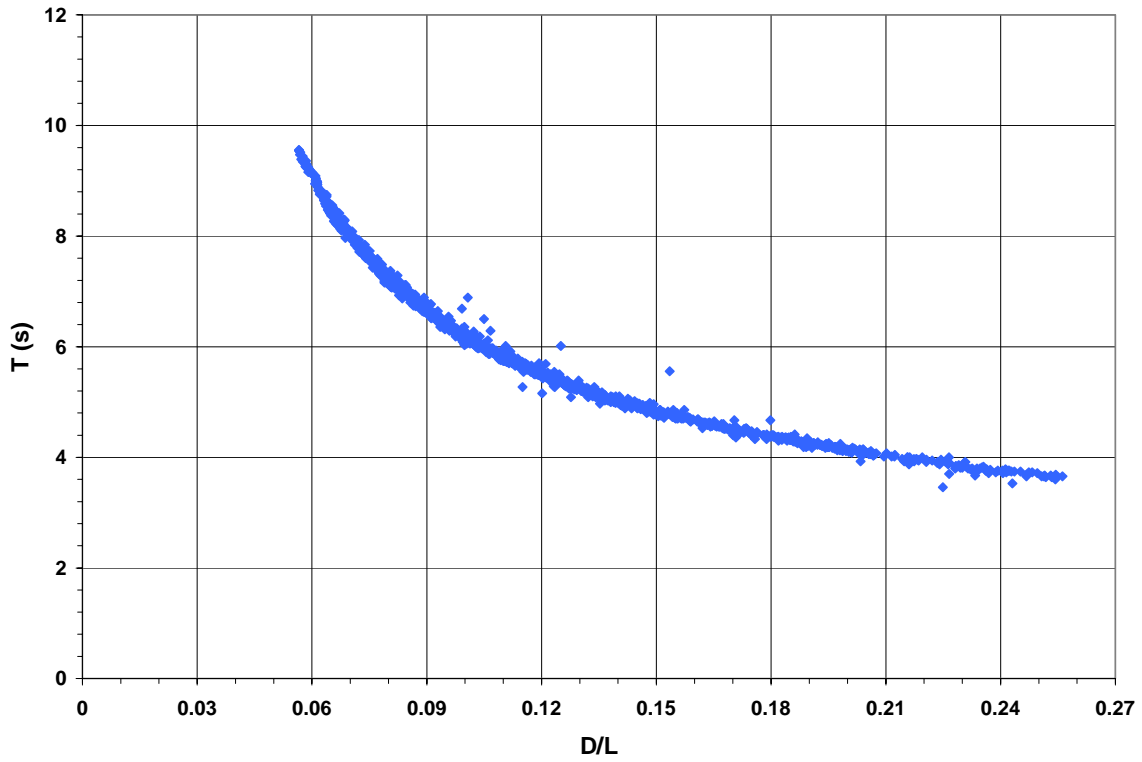


Figure 4.9 Wave period as a function of diffraction parameter, D/L.

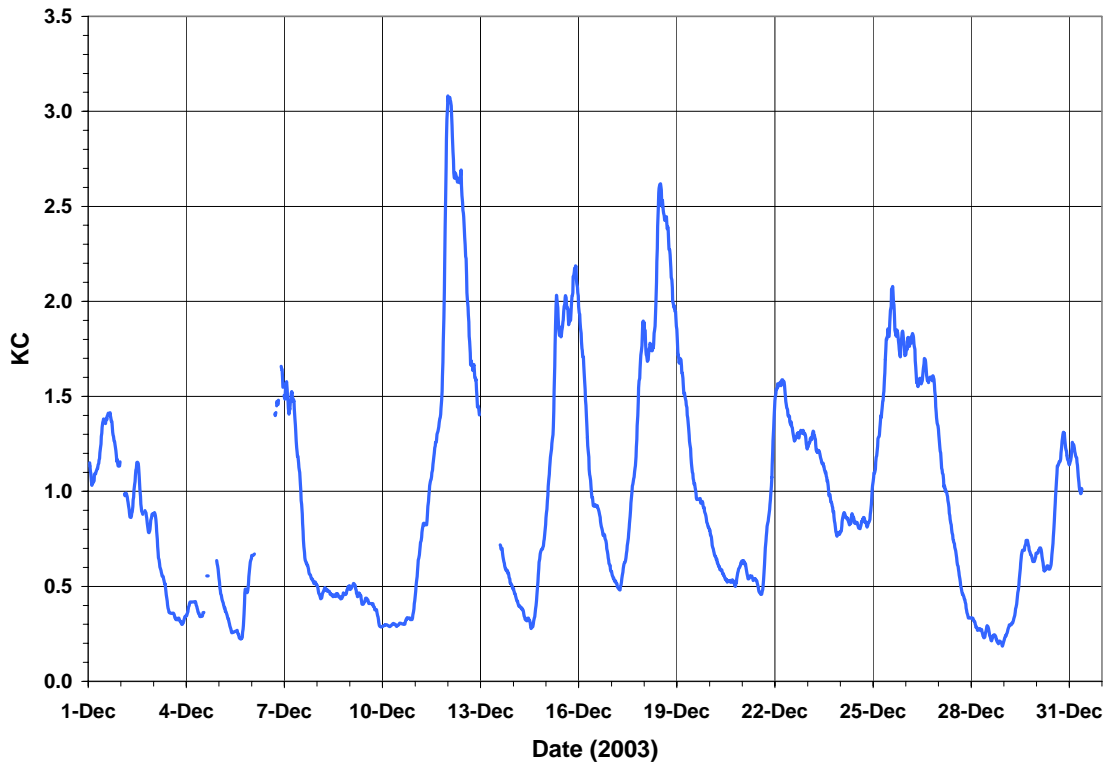
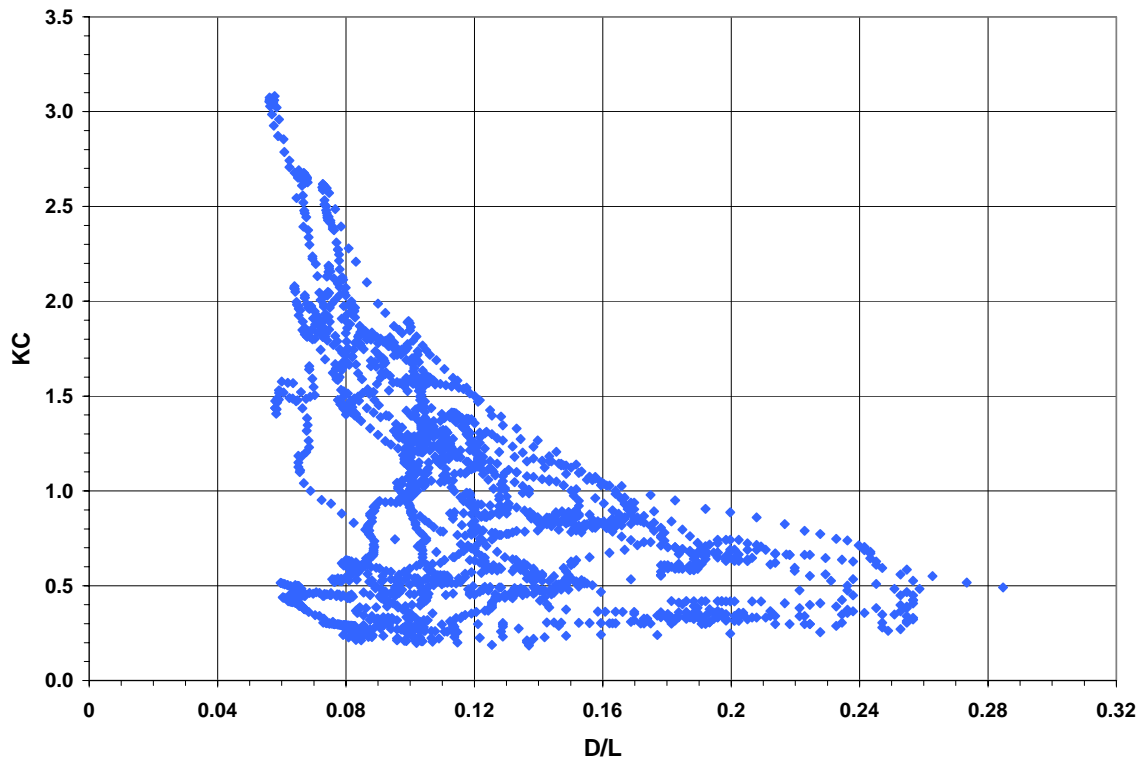


Figure 4.10 December 2003 time series of Keulegan-Carpenter number.



**Figure 4.11 Relationship of KC and D/L for December 2003 observations from MVCO site.**

Since, for any KC below 2.8, there is no separation zone with re-circulating vortices nor are there any shed vortices, potential flow analysis can be used to estimate the extent of changes in the flow expected from the influence of a pile to the wave induced velocities. The potential flow velocity in the radial direction is defined as (White, 1991)

$$V_r = U_\infty \left( 1 - \frac{R^2}{r^2} \right) \cos \theta$$

and, in the tangential direction as

$$V_\theta = -U_\infty \left( 1 + \frac{R^2}{r^2} \right) \sin \theta$$

where  $U_\infty$  is the free stream or undisturbed velocity,  $R$  is the pile radius,  $r$  is the radial distance from the center of the pile, and  $\theta$  defines the tangential direction clockwise from down stream. The speed is the magnitude of the vector components or

$$V = (V_r^2 + V_\theta^2)^{1/2}$$

Figure 4.12 shows the variation of potential flow velocity with respect to distance away from the pile in the down stream and cross stream directions. The velocity ratio is defined as the local velocity relative to the free stream or undisturbed velocity. At the pile surface, the downstream direction velocity ratio is zero but quickly rises to within 89 % of the free stream velocity in one pile diameter and to 99% within four pile diameters. In the cross stream direction, the velocity ratio is two at the pile but also quickly drops to within 11 % of the free stream velocity within one pile diameter and to 1 % within four pile diameters.

For a pile diameter of approximately 5.3 m (17.4 ft) this means that changes in flow velocity due to the pile will be very small within 5.3 m (17.4 ft) and insignificant within less than 20 m (66 ft). These results will scale the actual flow speeds, which are predicted by HYDROMAP to have maximum speeds at the alternative site of 0.25 to 0.5 m/s (0.5 to 1 kt).

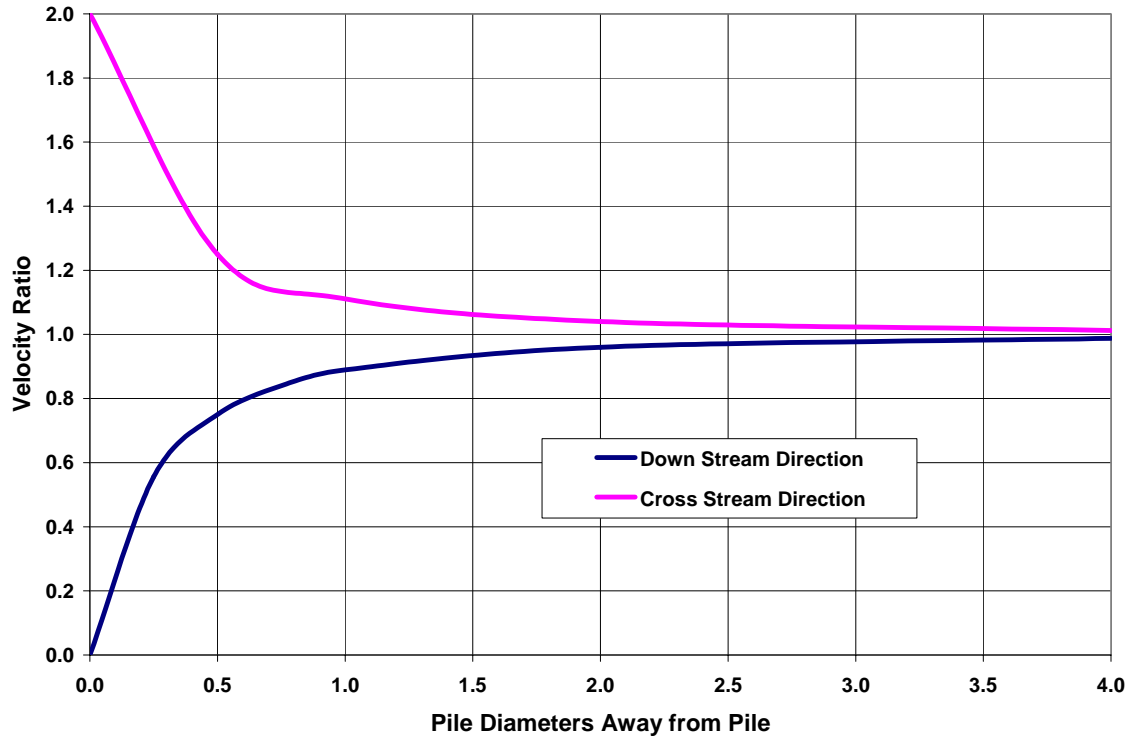


**Figure 4.12 Velocity variation based on potential flow in downstream and cross stream directions.**

The effects of tidal currents can also be examined with this approach since the tides are actually a long, shallow water wave. The wavelength for the tide wave in a water depth of 12 m (39 ft) and a period of 12.42 hrs or 44712 sec is approximately 480 km (300 mi). This gives a D/L of approximately zero. The Keulegan-Carpenter number can be calculated for a tidal wave assuming a tide range of 1 m (3.3 ft) to give a value of 3800. Thus the tide wave falls along the y-axis of Figure 4.1 in the zone where separation effects are important and vortices are shed from the pile. Note this value of KC negates the direct use of potential flow theory as given above but instead results in a vortex street downstream of the pile.

Following White's (1991) discussion of turbulent wakes, the velocity defect (defined as the difference between the free stream velocity and actual velocity behind the object) scales as  $x^{-2/3}$ , where  $x$  is the downstream distance from the cylinder (or pile), hence the effect dissipates rapidly.

In addition, Chakrabarti (1991) has shown through a systematic series of laboratory studies of cylinder groups in wave fields that wave forcing is independent of the spacing between cylinders if the spacing distance is greater than 5 for groups in line with the direction of wave propagation and 2 for groups perpendicular to the direction of wave propagation. These results are independent of the KC value. From extensive studies of the effects of pile spacing on scour, it has been shown that for pile spacings greater than two pile diameters, there is no difference in scour depth compared to the single pile case (Sumer and Fredsoe, 1998).

For the Cape Wind project, the pile spacing to diameter ratio is on the order of 100 to 200 based on pile diameters averaging 5.3 m (17.4 ft) and spacing from 630 to 1000 m (2070 to 3280 ft). Based on the results of the preceding analysis, there will then be no interaction in the wave and flow fields among the piles and the pile effects on waves and currents will be restricted to a zone of less than 5 pile diameters long (if not significantly shorter) and 2 diameters wide or less than 280 m<sup>2</sup> (3014 ft<sup>2</sup>). The total area for all 130 piles, less than 0.0364 km<sup>2</sup> (9 ac) can be compared to the total area of the wind farm of 71 km<sup>2</sup> (17,500 ac) showing that only 0.051% of the area of the wind farm is potentially affected. In reality, only a very small portion of this area is actually affected since all these impacts decrease quickly away from the pile.

### 4.3.2 Quad-Caisson Design

The quad-caisson design is a four-pile group with each pile at the corner of a square. Each pile has a diameter of 7.5 m (24.6 ft) and the side of the square, measured from pile centerlines is 29 m (95 ft). Based on extensive laboratory analyses the difference on scour due to currents and waves between the single pile and pile groups is the ratio of the gap between the piles to the individual pile diameter, G/D (Sumer et al., 2001). For waves and currents impinging on one face of the square the gap between piles is 21.5 m (70.5 ft). This gives a G/D ratio of 2.9. For waves and currents impinging on a corner of the square the projected gap between piles decreases to 13 m (42.7 ft). This results in a G/D ratio of 1.7.

Sumer and Fredsoe (1998) found through a series of laboratory studies that the smaller the G/D ratio the more significant the interference among the piles resulting in greater scour based on different pile group arrangements. Although they did not present the 2 x 2 pile arrangement of the quad-caisson, they found that, for a 2 pile arrangement no significant interference occurs for a G/D ratio greater than 2. For a 3 pile arrangement no significant interference occurs for a G/D ratio greater than 1. For a 4 x 4 pile arrangement no significant interference occurs for a G/D ratio greater than 1.5. Sumer et al., (2001) present results for a series of single, 2 x 2, 3 x 3 and 4 x 4 pile groups with a constant G/D ratio of 4. The 2 x 2 pile group shows an increase in scour depth of approximately 20% over the single pile results.

These results are also consistent with the design guidelines for estimating scour for pile groups in Richardson and Davis (2001). They present a methodology to estimate an equivalent single pile diameter for a pile group based on the angle of attack of the flow, the pile diameters and the pile spacing. For the quad caisson geometry, the projected equivalent pile diameter is 11.3 m (37 ft). This results in an equivalent pile diameter 2.1 times the diameter of the average monopile used in shallower water.

Assuming the analysis results for the monopile configuration presented in Section 4.3.1 can be extended for this larger equivalent monopile there is not a significant difference between the two. For instance the D/L ratio will approximately double (2.1) so the time series in Figure 4.7 will have a peak D/L of 0.59. Even though this maximum ratio indicates diffraction effects, it is due to small period and amplitude waves and is in deeper water where the quad caisson will be located, so the effect on sediment transport will still be insignificant. The time series presented in Figure 4.9 will essentially shift to the right indicating that waves for which diffraction is important (D/L > 0.2) have periods of < 6 sec. Although these waves constitute a higher percentage of observed waves, the substantial depth increase again more than offsets the potential for increase sediment transport. The Keulegan-Carpenter (KC) number will decrease with the larger equivalent pile diameter, from a mean of 0.96 for the monopile case to a mean of 0.46, dropping even further below the KC minimum where separation occurs (KC > 2.8).

The pile spacing to equivalent diameter ratio is on the order of 50 to 100 based on a pile diameter of 11.3 m (37 ft) and spacing from 630 to 1000 m (2070 to 3280 ft). Assuming the results of Section 4.3.1 for the monopile configuration apply to the equivalent monopile diameter estimated

from the quad-caisson configuration, there will then be no interaction in the wave and flow fields among the piles and the pile effects on waves and currents will be restricted to a zone of less than 5 pile diameters long (if not significantly shorter) and 2 diameters wide or less than 1280 m<sup>2</sup> (13,800 ft<sup>2</sup>). If one conservatively assumes that all 130 piles use the quad-caisson configuration for this site, less than 0.166 km<sup>2</sup> (41 ac) can be compared to the total area of the wind farm of 71 km<sup>2</sup> (17,500 ac) showing that only 0.23 % of the area of the wind farm is potentially affected. In reality, only a very small portion of this area is actually affected since all these impacts decrease quickly away from the pile.



## 5 Conclusions

A modeling and analysis study was performed to assess the probable effects of the WTG pile array from the Cape Wind Energy Project located at the alternative site southwest of Tuckernuck Island, just outside of Nantucket Sound, on waves and currents. Each WTG is either mounted on a monopile or a quad-caisson, consisting of four piles, depending on water depth. The monopile is between 5.1 and 5.5 m (16.75 and 18 ft) in diameter with the smaller diameter used in water depths from 3.6 to 12 m (12 to 39 ft) MLLW and the larger diameter used between depths of 12.2 to 15.2 m (40 to 50 ft). The quad-caisson consists of four piles 7.5 m (24.6 ft) in diameter tied together with cross members and connected to the tower supporting the WTG. The quad-caisson piles are located on the corners of a square 29 m (95 ft) on a side measured from the centerline of each pile. The quad-caisson design will be used in water depths from 15.2 to 27 m (50 to 90 ft). The study used a model, HYDROMAP, to calculate currents in the area and wave data was used that was acquired from MVCO for December 2003. This information was then used in a pile effects analysis to determine the zone of influence of each pile on waves and currents, whether adjacent piles would enhance the effects.

The HYDROMAP model was applied to the area offshore Massachusetts and Rhode Island to provide currents in the study area. Details of this application were reported in the analysis of the primary site on Horseshoe Shoal (Swanson et al., 2005).

The monopile analysis approach followed that typically used to evaluate the effects of offshore structures. The key parameters in these analyses are the diffraction parameter, which indicates whether a wave will diffract behind a pile and the Keulegan-Carpenter number, which indicates whether flow around the pile will separate and shed vortices in the downstream direction. Since both parameters require wave length, analysis of one month (December 2003) of wave data (wave height, wave period and water depth) was performed. Wave height ranged from 0.3 to 3.5 m (1 to 11.5 ft) with a mean of 1.4 m (4.7 ft). Wave period ranged from 3.5 to 9.5 sec with a mean of 6.0 sec. Wave length ranged from 19 to 94 m (62 to 308 ft) with a mean of 50 m (164 ft).

Diffraction effects were found to occur for only 4% of the waves from the time series. However the largest diffraction occurred for waves with the smallest period with low induced bottom velocities. These waves cause insignificant sediment transport regardless of whether they diffract or not and so can be ignored.

The calculation of the Keulegan-Carpenter number based on the wave data found no value greater than 3.1, which is only slightly above the threshold (2.8) for flow separation to occur. The mean KC value was approximately 0.96 (with a minimum of 0.19). KC is greater than 2.8 only 0.6 % of the month. The data primarily falls within the zone of insignificant separation effects (low KC) and insignificant diffraction (low D/L).

A potential flow analysis appropriate for this condition shows that the flow around the pile returns to within 89% of its undisturbed value within 1 pile diameter from the pile and to within 99% of its undisturbed value within 4 pile diameters. Using the same approach for the periodic tidal wave, a very long period shallow water wave, gave a large KC value of 3800, indicating that vortex shedding would occur. The velocity defect created by this vortex street dissipates rapidly, however, scaling at  $x^{-2/3}$ , where x is the distance downstream.

Comparison to laboratory studies of multiple piles indicates that there is no anticipated wake interaction among the piles since interaction ceases when the piles are spaced greater than five pile diameters from each other and the spacing for this project ranges from 120 to 190 pile

diameters. Using a single pile zone of influence of 5 pile diameters long (if not significantly shorter) and 2 diameters wide or less than 280 m<sup>2</sup> (3014 ft<sup>2</sup>), the total area for all 130 piles is less than 0.0364 km<sup>2</sup> (9 ac). This area can be compared to the total area of the WTG pile array on Horseshoe Shoal of 71 km<sup>2</sup> (17,500 ac) showing that only 0.051% of the area is potentially affected. In reality, only a very small portion of this area is actually affected since all these impacts decrease quickly away from the pile.

An analysis of scour around quad caisson configuration followed two approaches. The first looked at the literature for pile groups and found that the pile spacing to pile diameter (G/D) ratio was the critical parameter besides the KC number. The proposed quad caisson design ranged from 1.7 to 2.9 depending on the angle of the waves and currents impinging on the structure. Laboratory experiments showed that G/D ratios greater than 1 to 2, depending on pile group configurations, showed no interference effects among the piles. Thus for the most sensitive orientation of waves and currents oriented toward a corner of the quad caisson there may be an increased scour effect of approximately 20% over single pile results.

The second approach assumed that an equivalent monopile pile diameter can be calculated from a pile group based on the angle of attack of the flow, the individual pile diameter and the pile spacing. For the quad caisson geometry, the projected equivalent pile diameter is 11.3 m (37 ft). This results in an equivalent pile diameter 2.1 times the diameter of the average monopile used in shallower water. This approach resulted in a maximum possible pile effects area less than 1280 m<sup>2</sup> (13,800 ft<sup>2</sup>). If one conservatively assumes that all 130 piles use the quad-caisson configuration for this site, less than 0.166 km<sup>2</sup> (41 ac) can be compared to the total area of the wind farm of 71 km<sup>2</sup> (17,500 ac) showing that only 0.23 % of the area of the wind farm is potentially affected. Even though larger than the monopile results, the equivalent pile diameter approach still results in only a very small portion of the wind farm area is actually being affected.

## 6 References

- Chakrabarti, S. K., 1991, Waves forces on offshore structures, in Handbook of Ocean Engineering, Volume 2, John Herbich (editor), Gulf Publishing.
- Hunt, J. N., (1979) Direct solution of wave dispersion equation, Journal of Waterways, Ports, Coastal Ocean Division, ASCE, Vol.105, No.WW4, pp.457-459.
- Isaacson, M., 1979. Wave induced forces in the diffraction regime. In: Mechanics of Wave-Induced Forces on Cylinders. Ed. By T.J. Shaw, Pitman, San Francisco.
- Isaji, T.E., Howlett, C. Dalton and E. Anderson, 2001. Stepwise-continuous-variable-rectangular grid, in Proceedings of the 7th International Conference on Estuarine and Coastal Modeling, St. Pete Beach, FL, November 5-7, 2001.
- National Geophysical Data Center, 1998. GEophysical Data System for Hydrographic Survey Data, National Ocean Service, Ver. 4.
- National Geophysical Data Center, 2001. 2-Minute gridded global relief data, (October 2001) CD-ROM.
- Richardson, E.V. and S.R. Davis, 2001. Evaluating Scour at Bridges, 4<sup>th</sup> ed., Hydraulic Engineering Circular No. 18, Publication No. FHWA NHI 01-001, prepared for the Federal Highway Administration National Highway Institute.
- Sarpkaya, T. and M. Isaacson, 1981. Mechanics of Waves Forces on Offshore Structures. Van Nostrand Reinhold Company, New York.
- Sumer, B.M. and J. Fredsoe, 1998. Wave scour around group of vertical piles. Journal of Waterways, Port, Coastal Ocean Engineering, ASCE, Vol.124, No.5, pp.248-256.
- Sumer, B.M. and J. Fredsoe, 2002. The Mechanics of Scour in the Marine Environment. Advanced Series on Ocean Engineering – Volume 17. World Scientific, River Edge, New Jersey.
- Sumer, B.M., N. Christiansen, and J. Fredsoe, 1997. Horseshoe vortex and vortex shedding around vertical wall-mounted cylinder exposed to waves. J. Fluid Mechanics, vol. 332, 41-70.
- Sumer, B.M., R.J.S. Whitehouse, and A. Torum. 2001. Scour around coastal structures: a summary of recent research. Coastal Engineering, vol. 44, 153-190.
- Swanson, C. M. Spaulding, S. Sankar, and T. Isaji, 2005. Analysis of Effects of Wind Turbine Generator Oile Array of the Cape Wind Energy Project in Nantucket Sound. Submitted to Cape Wind Associates, LLC, Boston, MA, Submitted by Applied Science Associates, Inc., Narragansett, RI, ASA Draft Report 05-128.
- White, F.M., 1991. Viscous Fluid Flow. McGraw-Hill, Inc., New York.